



Original article

Active notch protects MAPK activated melanoma cell lines from MEK inhibitor cobimetinib

Letizia Porcelli^a, Annalisa Mazzotta^a, Marianna Garofoli^a, Roberta Di Fonte^a, Gabriella Guida^b, Michele Guida^c, Stefania Tommasi^d, Amalia Azzariti^{a,*}

^a Experimental Pharmacology Laboratory, Italia, 70124, Bari, Italy

^b Department of Basic Medical Sciences Neurosciences and Sense Organs, University of Bari, P.zza Giulio Cesare 11, 70124 Bari, Italy

^c Medical Oncology Unit, Italia, 70124, Bari, Italy

^d Molecular Diagnostics and Pharmacogenetics Unit IRCCS Istituto Tumori "Giovanni Paolo II" di Bari, Italia, 70124, Bari, Italy



ARTICLE INFO

Keywords:

Uveal melanoma
Senescence
Notch
MEK

Chemical compounds studied in this article:

Cobimetinib (PubChem CID: 16222096)

Nirogacestat (PubChem CID:46224413)

ABSTRACT

The crosstalk between Notch and MAPK pathway plays a role in MEK inhibitor resistance in BRAF^{V600E} metastatic melanoma (MM) and promotes migration in GNAQ^{Q209L} uveal melanoma (UM) cells. We determined the cytotoxicity of combinatorial inhibition of MEK and Notch by cobimetinib and γ -secretase inhibitor (GSI) nirogacestat, in BRAF^{V600E} and BRAF wt MM and GNAQ^{Q209L} UM cells displaying different Erk1/2 and Notch activation status, with the aim to elucidate the impact of Notch signaling in the response to MEK inhibitor. Overall the combination was synergic in BRAF^{V600E} MM and GNAQ^{Q209L} UM cells and antagonistic in BRAF wt one. Focusing on UM cells, we found that cobimetinib resulted in G0/G1 phase arrest and apoptosis induction, whereas the combination with GSI increased treatment efficacy by inducing a senescent-like state of cells and by blocking migration towards liver cancer cells. Mechanistically, this was reflected in a strong reduction of cyclin D1, in the inactivation of retinoblastoma protein and in the increase of p27^{KIP1} expression levels. Of note, each drug alone prevented Notch signaling activation resulting in inhibition of c-jun(Ser63) and Hes-1 expression. The combination achieved the strongest inhibition on Notch signaling and on both c-jun(Ser63) and Erk1/2 activation level. In conclusion we unveiled a coordinate action of MAPK and Notch signaling in promoting proliferation of BRAF^{V600E} MM and GNAQ^{Q209L} UM cells. Remarkably, the simultaneous inhibition of MEK and Notch signaling highlighted a role for the second pathway in protecting cells against senescence in GNAQ^{Q209L} UM cells treated with the MEK inhibitor.

1. Introduction

Unraveling the mechanisms by which melanoma can be triggered and sustained is crucial. Mitogen activated protein kinase (MAPK) signaling is an evolutionarily conserved signal transduction pathway, including at least seven MAPKs [1], which ultimately drive the activation of ERK, JNK, or p38 MAPKs, each of them promoting a variety of physiological programs such as proliferation, differentiation, development, migration, apoptosis, and transformation of cells [1,2]. In particular, transient activation of ERK can induce melanocyte differentiation [3], while sustained activation, by mitogenic stimuli, promotes melanocytes proliferation. Mitogenic stimuli in about half of all metastatic melanoma (MM) are triggered by mutations in BRAF gene (BRAF V600), which stimulates the growth of cancer cells through the

activation of the MAPKs MEK1/2 [4]. For such patients the gold standard is therefore a combination therapy with BRAF inhibitor (BRAFi) and MEK inhibitor (MEKi) [5], which additionally delays the onset of resistance that invariably develops in such patients [6,7]. The remaining MM patients are BRAF wild-type, that do not benefit from BRAF/MEK inhibitors treatment and, despite they carry a wide spectrum of candidate mutations to be targeted, their treatment is still a challenging problem [8]. In uveal melanoma instead, about 80 % of cases harbour one of the mutually exclusive activating mutations in GNAQ (*guanine nucleotide binding-protein G(q) subunit alpha*) or its paralogue guanine nucleotide-binding protein subunit alpha-11 (*GNA11*) genes [9–11], which render the heterotrimeric G protein α subunits G α q and G α 11 GTPase constitutively active [12]. The best-known downstream signaling event, initiated by G α q, involves the activation of

* Corresponding author at: Experimental Pharmacology Laboratory - IRCCS Istituto Tumori Giovanni Paolo II, Viale O. Flacco, 65 - 70124 Bari, Italy.

E-mail address: a.azzariti@oncologico.bari.it (A. Azzariti).

<https://doi.org/10.1016/j.bioph.2020.111006>

Received 7 April 2020; Received in revised form 26 October 2020; Accepted 8 November 2020

Available online 14 November 2020

0753-3322/© 2020 The Authors.

Published by Elsevier Masson SAS. This is an open access article under the CC BY-NC-ND license

(<http://creativecommons.org/licenses/by-nc-nd/4.0/>).

phospholipase C- β (PLC- β), leading through a cascade mechanism to the constitutive activation of MAPK signaling pathway [13]. Therefore, the efficacy and safety of MEKi has been evaluated in clinical trials on metastatic UM patients [www.clinicaltrials.gov], though reporting disappointing results as well as other pharmacological approaches such as immunotherapy which instead results effective in cutaneous melanoma [14]. Growing evidences have suggested Notch signaling as one of the most important pathway in drug-resistant tumour cells [15] and in melanoma progression [16]. Notch signaling cascade belongs to evolutionally conserved signaling pathways with a crucial role during both embryonic and postnatal development [17]. Beside its fundamental role in keratinocyte differentiation, Notch is fundamental for the regulation of melanocyte lineage development [18], however Notch activation is a driving event in melanocytic transformation and melanoma progression [16,19,20], including uveal melanoma [21,22]. Notch signaling is triggered by direct interactions between membrane-bound Notch receptors (Notch1-4) on the receiver cells and Notch ligands (Delta-like or Jagged) on the sender cells [23]. Upon activation, Notch receptor intracellular domain (NICD) is released by the proteolytic cleavage of γ -secretase and moves into the nucleus where it plays its biological functions as transcriptional regulator [23–25]. Liu et al. reported that mutant *GNAQ* contributed to the activation of Notch signaling, whereas its inhibition prevented the stimulatory effect of *GNAQ* on cell viability and migration of UM cells [21]. Remarkably, a large body of evidence has highlighted the importance of Notch-Ras cooperation in the pathogenesis of several cancers. In breast cancer a coordinate hyperactivation of Notch1 and Ras/MAPK pathways has been identified as a biomarker of poor prognosis [26–28]. Accordingly Tremblay et al., have shown that MEK/ERK pathway promotes Notch signaling in pancreatic cancer cells [29], whereas Nishikawa et al. have reported that Hes1, which is transcriptionally activated by Notch signaling, plays an essential role in KRAS-driven pancreatic tumorigenesis [30]. Of note, Notch signaling is among signaling cascade with potential to confer resistance to anti-MAPK therapy, as demonstrated in *BRAF*-mutated melanoma [31]. Additionally a constitutive activation of Notch prevented the oncogene-induced senescence in *BRAF*^{V600E} and *NRAS*^{Q61R} melanoma cells [32], hereby promoting the malignant transformation of melanocytes. Moreover, the combination strategies with Notch antagonists maximized the efficacy of MAPK inhibition in *BRAF* mutated melanoma and, remarkably, Notch receptors were found differentially expressed in responder and non-responder melanomas [33]. Based on this background, here we hypothesized the cooperation between Notch and MAPK signaling in driving proliferation and responsiveness to MEKi of melanoma cells. Therefore the aim of this study was to identify among melanoma cell lines, including cutaneous MM *BRAF* wild type, MM *BRAF*^{V600E} and uveal melanoma cell line carrying *GNAQ*^{Q209L}, those with a constitutive activation of Notch and/or MAPK signaling to test the potentiality of a MEKi/ γ -secretase inhibitor (GSI)-based combination therapy.

2. Materials and methods

2.1. Chemicals

MEK inhibitor cobimetinib, was purchased from Selleckchem (Munich, Germany). It was dissolved at 865 mM in dimethylsulfoxide (DMSO) and then it was stored in aliquots at -20°C . The inhibitor of the γ -secretase inhibitor (GSI) nirogacestat, also designated as PF-03084014, was graciously supplied by Pfizer Inc., USA. Afterwards it was dissolved in DMSO at 10 mM and stored in aliquots at -20°C .

2.2. Cell culture

The UM cells 92.1 were commercially obtained from ICLC, by Prof. Ragusa (University of Catania, Catania, Italy and Oasi Research Institute - IRCCS, Troina, Italy) and then generously gifted to us. Hmel-1 and M3

MM cells (from human sporadic *BRAF*^{V600E} melanoma biopsy specimens) were established from us and characterized as reported in Zanna et al. [34]. LND-1 and HBL MM cells (*BRAF* wild type) were gifted to us by Prof. G. Ghanem, University of Bruxelles. All Cells were cultured in vitro in high glucose Dulbecco's modified Eagle's medium (DMEM) supplemented with 10 % (v/v) fetal bovine serum (FBS), 1% (v/v) L-glutamine, and 1% (v/v) penicillin/streptomycin, and at 37°C in a humidified atmosphere at 5% CO_2 . HepG2 liver cancer cells were kindly provided to us by Prof. G. Giannelli [35,36]. The latter cells was cultured in RPMI 1640 supplemented with 10 % (v/v) FBS, 1% (v/v) L-glutamine, and 1% (v/v) penicillin/streptomycin at 37°C in a humidified atmosphere at 5% CO_2 . For the experiments the cells within 4–8 passages were utilized after routinely testing for mycoplasma contamination.

2.3. Cell viability assays and combination index analysis

To evaluate the cytotoxic activity of single drug, the inhibitory effect on cell growth by cobimetinib and nirogacestat was evaluated using the 3-(4,5-dimethylthiazol-2-yl)-2,5-diphenyltetrazolium (MTT) assay after 72 h of treatment. For this purpose, cells were plated in 100 μL medium, in 96 plates at a density of 7500 per well. After 24 h attached cells were exposed to various concentrations of cobimetinib and nirogacestat alone or in combination. In each plate, one column contained cells which were not exposed to any drug (vehicle-treated cells), while each drug concentration was repeated in 6 identical wells. After three days, the results of the growth inhibition were expressed as dose-effect curves with a plot of the fraction of unaffected (surviving) cells versus drug concentration. The IC_{50} was defined as the concentration of drug resulting in a 50 % inhibition of cell proliferation vs vehicle treated cells and was calculated utilizing CalcuSyn ver.1.1.1 software (Biosoft, UK). The combination index (CI) values were calculated for all tested drug concentrations according to the Chou and Talalay method [37]. The CI theorem provides quantitative definition for additive effects (CI = 1), synergism (CI < 1) and antagonism (CI > 1) in drugs combinations.

2.4. Cell cycle analysis

Cell cycle modulation induced by treatments (cobimetinib and nirogacestat alone or in combination at 0.05 μM and 2.5 μM , respectively) for 24 h and 48 h was studied by propidium iodide (PI) staining and flow cytometry analysis by using a FACScan (BD Biosciences, US). After two wash steps in ice-cold PBS (pH 7.4), the cells were fixed in 4.5 mL of 70 % ethanol and stored at -20°C . For the analysis, the pellet was resuspended in PBS containing 1 mg/mL RNase, 0.01 % NP40 and 50 $\mu\text{g}/\text{mL}$ PI (Sigma). After an incubation time of 30 min in ice, cell cycle analysis was performed. Data were interpreted by using the Cell Quest software (BD Biosciences, US), provided by the manufacturer.

2.5. Cell apoptosis assay

The Annexin V-FITC Apoptosis Detection Kit (BD Biosciences, US) was used to detect apoptosis by flow cytometry [38]. The cells were exposed to the drugs (cobimetinib and nirogacestat alone or in combination at 0.05 μM and 2.5 μM , respectively) and after 24–48 h they were harvested and processed according to the manufacturer's instructions. Data are presented as the calculated fractions of Annexin V and PI-positive cells in the 92.1 treated vs vehicle treated cells (Ctrl).

2.6. Cellular effectors analysis

The cells were exposed to cobimetinib and nirogacestat alone or in combination (at 0.05 μM and 2.5 μM , respectively) and protein expression was analyzed by Western Blotting. After 24 h of treatments, protein extracts were obtained by homogenization in Cell Lyses buffer (20 mM Tris-HCl (pH 7.5), 150 mM NaCl, 1 mM Na_2EDTA , 1 mM EGTA, 1% Triton, 2.5 mM sodium pyrophosphate, 1 mM beta-

glycerophosphate, 1 mM Na₃VO₄, 1 µg/mL leupeptin) and a protease inhibitor cocktail (P2714, Sigma-Aldrich) in the presence of 1 mM phenylmethylsulfonyl fluoride (PMSF). Total proteins were measured by Bradford method and 50 µg were electrophoretically separated on 10 % acrylamide gel (SDS-PAGE by Laemli). After the transfer onto PVDF membranes, the immunoblotting was performed by using specified primary antibodies against: p21 Waf1/Cip1 (dilution 1:1000; #2947, Cell Signaling), phospho-Rb (Ser795) (dilution 1:1000; #9301, Cell Signaling), Cyclin D1 (dilution 1:1000; #3686, Cell Signaling), CDK6 (dilution 1:2000; #3136, Cell Signaling), CDK4 (dilution 1:1000; #12790, Cell Signaling), NOTCH1 (dilution 1:1000; #3608, Cell Signaling), NOTCH2 (dilution 1:1000; #5732, Cell Signaling), NOTCH3 (dilution 1:1000; #5276, Cell Signaling), HES1 (dilution 1:1000; #11988, Cell Signaling), phospho-c-Jun (Ser63) (dilution 1:1000; #2361, Cell Signaling), p44/42 MAPK (Erk1/2) (dilution 1:1000; #9102, Cell Signaling), phospho-p44/42 MAPK (Erk1/2) (Thr202/Tyr204) (dilution 1:1000; #9106, Cell Signaling), β-actin 1:10000, Sigma-Aldrich. The secondary antibodies were anti-rabbit-HRP or anti-mouse-HRP (GE Healthcare Life Sciences). Blots were viewed and analyzed using ChemiDoc XRS and the Quantity One software (Bio-Rad); β-actin expression levels were used to normalize the sample values.

2.7. Real-Time PCR

To investigate the effects of the drugs on expression of *NOTCH-1*, *NOTCH-2*, *NOTCH-3*, *HES-1*, and *CCND1*, the 92.1 cells were treated with cobimetinib (0.05 µM), niraparicestat (2.5 µM), and combination of both (0.05 µM of cobimetinib + 2.5 µM of niraparicestat) for 24 h. The treated cells were then harvested and total RNA was extracted using TRIzol reagent (Thermo Fisher Scientific) and used for synthesis of cDNA by High Capacity cDNA Reverse Transcription Kit (Applied Biosystems™). Relative expression of *NOTCH-1*, *NOTCH-2*, *NOTCH-3*, *HES-1* and *CCND1* mRNA were then measured in a StepOnePlus™ Real-Time PCR System (Applied Biosystems™), by using specific primers for each gene and PowerUp™ SYBR™ Green Master Mix mRNA quantitative real-time polymerase chain reaction Kit (Applied Biosystems™). Forward (F) and reverse (R) specific primer sequences for each gene are shown in the Additional File 1. Gene expression was normalized to the level of glyceraldehyde-3-phosphate dehydrogenase (*GAPDH*) within each sample using the relative ΔΔCT method.

2.8. Senescence and proliferation assay

For senescence assay 92.1 cells were plated in 60 mm dishes at a density of 2.5×10^5 /dish and the next day they were treated with niraparicestat and cobimetinib as single treatment and in combination. After three days treatment, the cells were washed and leave to stand in drug-free medium for additional 4 days. Then, the cells were fixed for 15 min in β-galactosidase fixative, washed with PBS and stained in β-galactosidase staining solution at 37 °C until β-galactosidase staining (blue color) became visible at optical observation. For proliferation assay 92.1 cells were plated into 12-well plates at $65-70 \times 10^3$ cells/plate and then incubated at 37 °C with CO₂. After three days from treatments (as reported before), the medium of cells was carefully removed and replaced with the fresh medium for additional four days. After two washing steps, the cells were fixed with methyl alcohol for 30 min, stained with 0.1 % crystal violet solution for 30 min, and examined by inverted microscope.

2.9. Transwell migration assay

The migration assays were performed in 24-well cultured plates with 8 µm pore size transwell chamber inserts (Lifescience). Chemotactic cells (2×10^5 cells/well) HepG2, were added to the bottom chambers of 24-well culture plates and incubated for 24 h. Then, the culture medium was replaced by DMEM containing 0,2% FBS and 92.1 tumor cells suspension (4×10^4 / mL) was added to the upper compartment in DMEM

containing 0,2% FBS, while the cells in the upper and bottom chamber were not in contact. When the cells in the upper compartment were adhered to the transwell, the drugs (cobimetinib at 0.05 µM, niraparicestat at 2.5 µM and the combination of 0.05 µM cobimetinib / 2.5 µM niraparicestat) were added. After incubation at 37 °C / 5% CO₂ for 24 h, the non-migrated cells that remained on the upper surface of the membrane were scraped. The migrated cells on the lower face of the membrane were fixed with methanol and stained with the Diff-Quick staining method. Migrating cells were observed under a light microscope from 10 random fields at 200x magnification for each triplicate sample to get pictures which represented the biological effect.

2.10. Wound healing assay

To further evaluate cell migration in response to drug treatment, confluent monolayer of 92.1 cells were wounded and treated with cobimetinib at 0.05 µM, niraparicestat at 2.5 µM and with the drugs combination, or left untreated (vehicle treated cell). The plates were photographed at time 0 and after 24 h post wounding and the Migration Rate was quantified by dividing the change in wound width by the time spent in migration, using the following equation $RM = \frac{Wi - Wf}{t}$, [RM = Rate of cell migration (nm/h), Wi = initial wound width (nm), Wf = final wound width (nm), t = duration of migration (hours)], as reported by Grada et al. [39]. The wound width at time 0 and at time 24 h was determined by manual quantification of the distance between the edges of the scratch. The experiment was conducted in triplicate samples.

2.11. Statistical analyses

All experiments were carried out in triplicate, unless otherwise indicated, and data are presented as the mean ± standard deviation (SD). P values, calculated by the two-tailed *t*-test, lower than 0.05 were considered statistically significant. Statistical calculations were carried out using GraphPad Prism 5.0 software (GraphPad Software Inc., San Diego, CA, USA).

3. Results

3.1. Synergistic growth repression upon MEK and Notch signaling inhibition

In order to evaluate the activation status of Notch and MAPK pathways, we determined the expression of Notch1-NTM, Hes-1 and Erk1/2 phosphorylation level in melanoma cells included in the study (Hmel-1, M3, HBL, LND-1 and 92.1). Such analysis, evidenced that i) Notch1 signaling was activated in 92.1 uveal melanoma cells to higher extent compared to the other cell lines tested; indeed the expression level of Notch1-NTM was the lowest and that of Hes-1 was the highest, and ii) MAPK signaling was instead activated at highest extent in BRAF^{V600E}, Hmel-1 and M3 (i.e. highest level of p-Erk1/2), followed by 92.1 and BRAF wild type cells (Fig. 1a). To evaluate whether active Notch influenced the response to MEKi, we tested the antitumor efficacy of the combined inhibition of MEK and Notch signaling in 92.1 cell line, as a representative model carrying the highest activation of both Notch and p-Erk1/2 signaling, in Hmel-1 cell line such as the one with the highest activation of p-Erk1/2, and in HBL cell line as representative one of lowest activation of both signaling pathways. To this purpose, after the determination of the concentration of drugs yielding 50 % inhibition of cell growth (IC₅₀) for cobimetinib and niraparicestat (reported in Fig. 1b), the drugs were simultaneously administered in scalar concentrations as reported in Materials and Methods section. At each dose utilized, the combination of drugs showed to be more effective than each drug alone in 92.1 and Hmel-1 cells. Indeed the combination index (CI), evaluated according to the Chou and Talalay method [37], showed that it was synergic for all tested drugs concentrations in Hmel-1 and in 92.1 cell

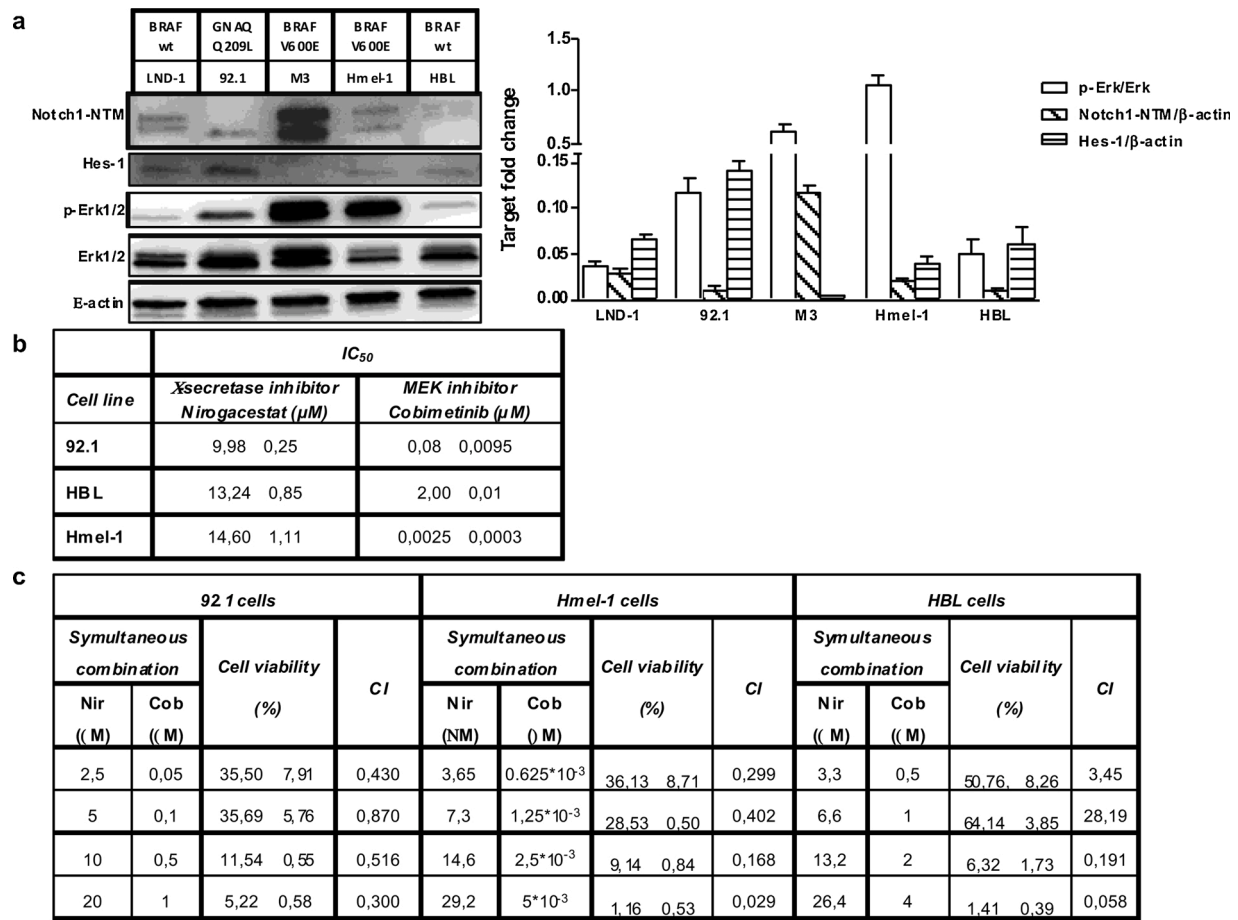


Fig. 1. i) Characterization of p-Erk1/2/Erk1/2 and Notch1 signaling activation in tumor cells included in the study. a. Electrophoretic bands of Notch1-NTM, Hes-1, p-Erk1/2 and β -actin in all melanoma cell lines are showed with the histogram plot reporting Notch1-NTM/ β -actin, Hes-1/ β -actin, p-Erk1/2 / Erk1/2 expression level ii) Determination of drugs IC_{50} . b. Table reporting 72 h- IC_{50} values for cobimetinib and nirogacestat obtained in 92.1, HBL and Hmel-1 cell lines, iii) Evaluation of pharmacological interaction between drugs. c. Table reporting the Combination Index (CIs) for four combinations of drugs concentrations. All data reported are the means \pm SD from three independent experiments. The significance of differences was analyzed with two tailed t-test and are reported in Fig. 6S.

lines, while it was antagonist or synergic in HBL, depending on drugs concentrations utilized (data reported in Fig. 1c). The dose/effect/ plots for each drug and drugs combination together with the combination index (CI) plots, are reported in Fig. 1S. Because such combination has already been evaluated in BRAF mutated MM cells [33] and uveal melanoma cells displayed the highest sensitivity to GSI, according to the activation of Notch1 signaling in such cells, we decided to continue our study on UM cells to shed light on possible mechanisms, driven by Notch signaling, counteracting the response to MEKi in uveal melanoma cells. Therefore all following experiments were carried out in 92.1 cells by using concentrations of drugs (0.05 μM and 2.5 μM for cobimetinib and nirogacestat, respectively) yielding a CI = 0.4, and that represented the lowest doses responsible for more than 50 % inhibition of cell proliferation.

3.2. Combining MEKi and GSI caused the exit from cell cycle of GNAQ^{Q209L} 92.1 cells

To determine whether the inhibition of cell proliferation was through the affection of cell cycle progression, we treated the cells with each drug and with drugs combination and then we assessed cell cycle distribution after 24 h. We found that nirogacestat slightly affected G0/G1 and the S-phase cells fractions, whereas cobimetinib increased the first of almost 10 % and reduced the second of almost 50 %, meaning that MEKi maintained cells in a quiescent state. The combination further increased the arrest caused by cobimetinib at the G0/G1-phase (20 % vs

10 % of cobimetinib-treated cells) and reduced the S-phase fraction (60 % vs 50 % of cobimetinib treated cells), resulting in the almost complete exit of cells from cell cycle (91.6 % arrested cells at G0/G1). A representative output file of cell cycle analysis is reported in Fig. 2a whereas the corresponding histograms plot, reporting the percentage of cell cycle phases obtained from three independent experiments, is reported in Fig. 2b.

3.3. Combining MEKi and GSI induced a senescent-like state rather than apoptosis in 92.1 cells

The induction of apoptosis was evaluated as a consequence of 24 and 48 h of treatment with each drug and their combination, by determining the fraction of Annexin V and Annexin V/PI positive cells in treated cells vs vehicle treated ones. Nirogacestat caused one-fold increase of Annexin V positive cells, meaning induction of early apoptosis after 24 h. Cobimetinib instead, caused a four-fold increase of Annexin V positive cells, while the drugs combination did not further increase the extent of early apoptosis induced by MEKi. A representative analysis is reported in Fig. 3a, whereas the corresponding histogram plot, reporting the fold change of both Annexin V and Annexin V + PI positive cells (early + late apoptosis) vs vehicle treated cells (Ctrl), obtained from three independent experiments, is reported in Fig. 3b (*p < 0.05).

Single drug and the combination did not significantly increase the amount of apoptosis after 48 h of treatment. However the latter induced a partial shift from Annexin V positive cells to Annexin V/PI positive

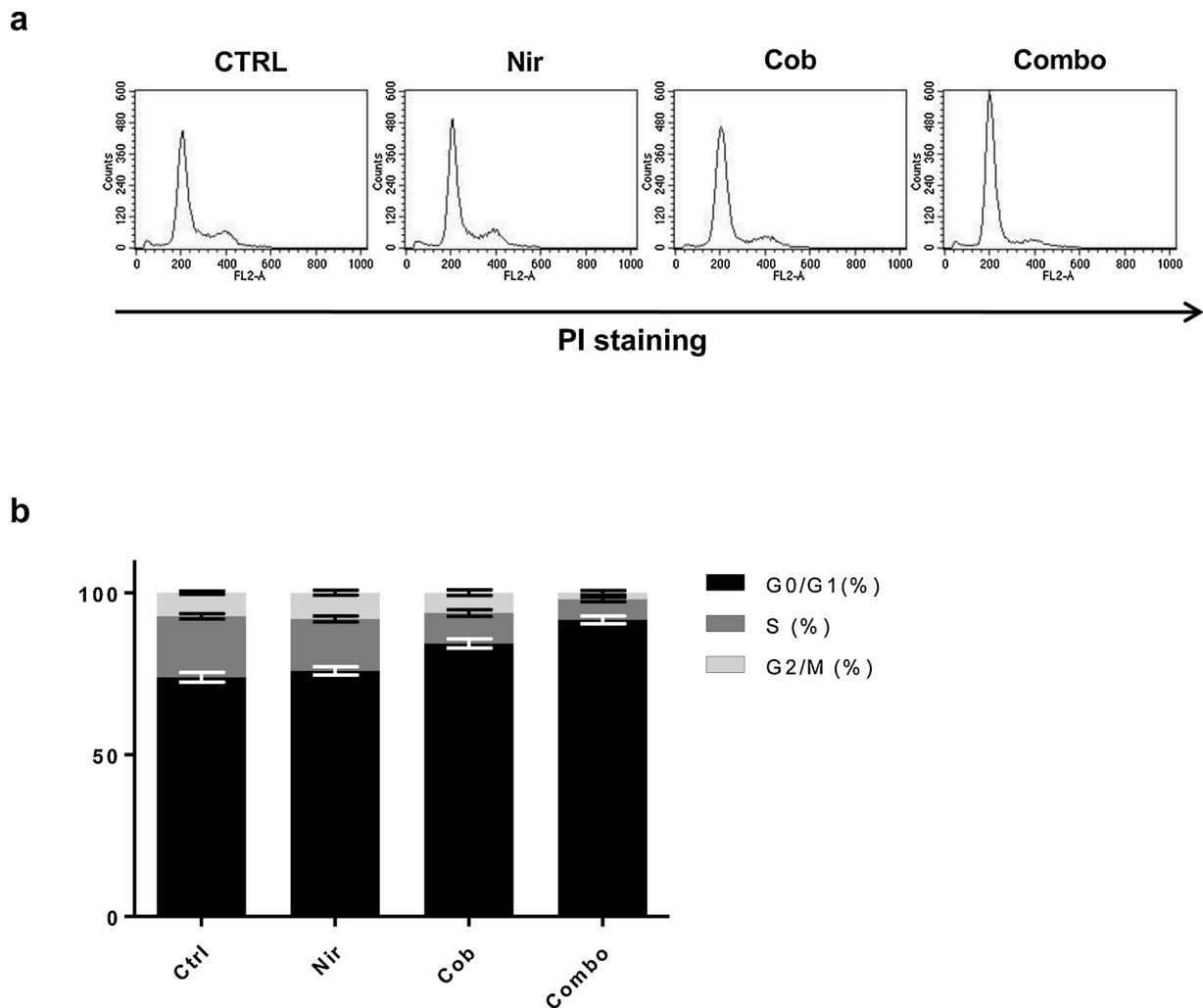


Fig. 2. The combination induced cell cycle arrest at G0/G1 in 92.1 cell line. a. Flow cytometry profile of cell cycle by single drug and combination after 24 h of treatments. b. Histograms of cell cycle phases after 24 h of drug treatment evidencing the arrest at G0/G1 phase and the reduction of S-phase induced by drugs combination and by single drug. The data reported are means \pm SD from three independent experiments. SD values of each mean are in the range 1-2 % and the significance of differences was analyzed with two tailed *t*-test and reported in Fig. 7S.

cells, meaning progression from early to late apoptosis (such data are reported in Fig. 2S). Because drugs combination markedly increased treatment efficacy, albeit it did not induce an increase of apoptosis, we speculated that in the majority of cells a prolonged arrest at G0/G1 phase (evidenced in cell cycle analysis) led to a senescent-like state which suppressed cell proliferation. To ascertain if the drugs combination led to senescence, we challenged the cells with each drug and their combination, afterwards the cells were washed and cultured in drug-free medium for additional four days and then stained with crystal violet or assayed for a senescence-associated expression of β -galactosidase (SA- β -Gal). Such evaluations demonstrated that by inhibiting Notch, an irreversible repression of cell proliferation occurred, showing that such signaling pathway promoted cell growth and protected 92.1 GNAQ mutated cells against senescence. The optical examination of GSI-treated cells further confirmed the phenotypic changes consistent with quiescent and senescent state [40], because of blue color development due to SA- β -Gal. Of note, this assay highlighted that MEKi instead resulted in a reversible inhibition of cell proliferation since the cells started to re-growth in drug-free medium, appeared similar to vehicle treated cells and no SA- β -Gal staining was found. The combination of GSI with MEKi achieved the highest therapeutic efficacy, as demonstrated by the morphological examination of cells and by the increased SA- β -Gal staining in specimens, coherent with cells that have lost the chance to

re-start proliferation after a prolonged quiescent state. Representative pictures of three independent experiments performed for cell proliferation evaluation, morphological state assessment and for development of SA- β -Gal are reported in Fig. 4.

3.4. Combining MEKi and GSI unveiled a cooperative mechanism between MAPK and Notch pathway to promote cell proliferation

In order to determine the underlying mechanisms leading to cell growth inhibition and induction of senescence, we focused on cell targets related to cell cycle progression and proliferation. The G1-S phase transition is tightly regulated by D-type cyclin levels, which limit the activity of CDK4/6 and by inhibitory proteins like p27^{KIP1} and p21^{CIP1}, which potently prevent CDK4/6-mediated phosphorylation of retinoblastoma protein (RB), thus resulting in the repression of E2F target genes expression and cell cycle arrest [41]. Because of the expression of GNAQ^{Q209L} in 92.1 cells, the activation of mitogenic stimuli was markedly evident by endogenous Erk1/2, c-jun phosphorylation and cyclin D1 expression level. Notch pathway was constitutively activated, as showed by high levels of endogenous Hes-1, as already demonstrated by Asnaghi et al. in 92.1 cells [42]. Compared to vehicle-treated cells, nirogacestat, by inhibiting gamma secretase complex, resulted in significant reduction of Notch1 receptor processing and activation, as

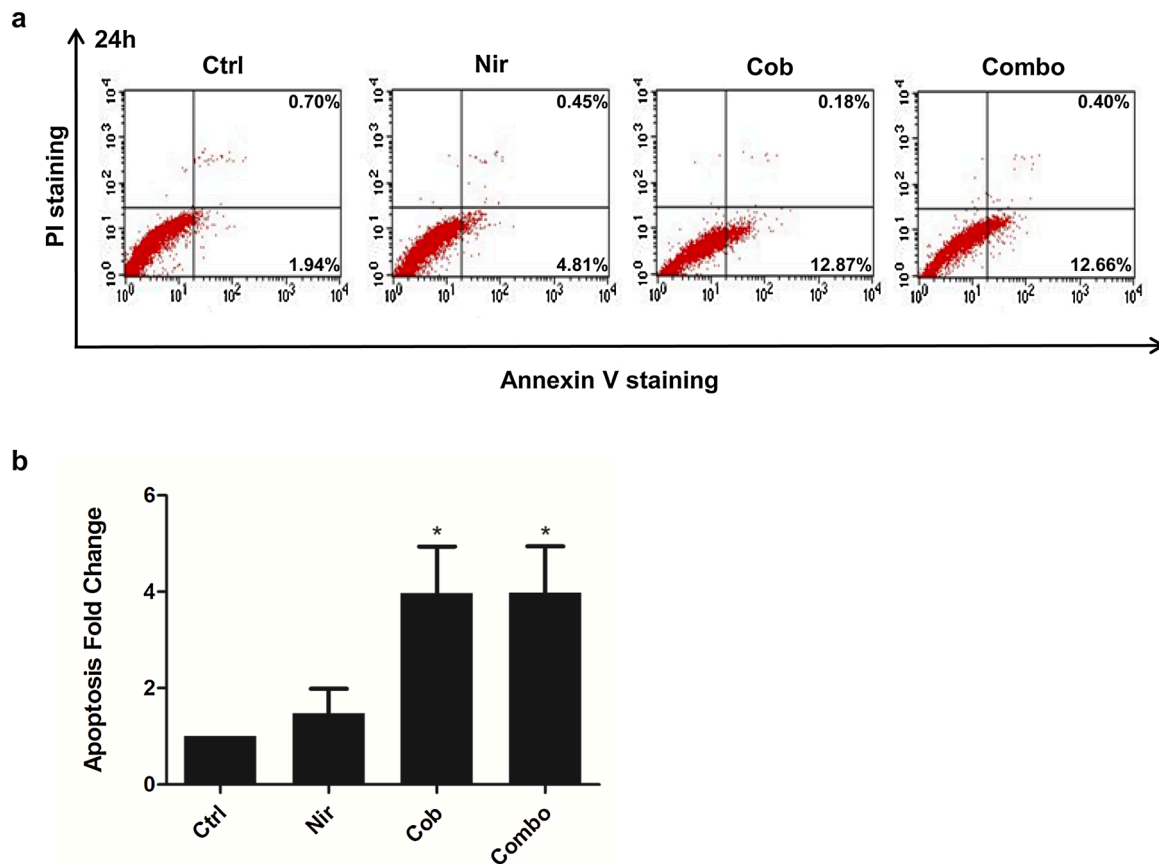


Fig. 3. Drugs combination induced apoptosis in 92.1 cells to the same extent as cobimetinib. a. Dot plots reporting a representative analysis by FACS. b. Histogram plot reporting mean value \pm SD from three independent experiments and expressing the fold change of apoptosis induction in drug(s)-treated vs vehicle treated cells (Ctrl). Two tailed *t*-test was used to analyze the difference between treated cells vs vehicle treated ones (**p* < 0.05).

confirmed by increased expression of Notch1-NTM, consisting of the trans-membrane and intracellular part of Notch receptor (ICN). Blockade of Notch1 was accompanied by a significant reduction of p-c-jun(Ser63) and Hes-1 vs vehicle treated cell (Ctrl). Erk1/2 phosphorylation instead, was significantly increased, whereas neither cyclin D1 and p27 expression level, nor RB protein phosphorylation were modulated, according to the status of cell cycle after nirogacestat (reported before). Of note, compared to vehicle-treated cells, the administration of cobimetinib resulted in a significant inhibition of Notch1/3 receptors activation, which caused the decrease of Hes-1 expression, the reduction of p-c-jun(Ser63) and cyclin D1 expression level. Erk1/2 phosphorylation was not reduced by tested concentration of cobimetinib, whereas p27 expression and RB protein phosphorylation levels were significantly increased and reduced, respectively, according to the arrest at G0/G1 phase induced by the drug (reported before). Such results clearly suggested that a strong cooperation between Notch/JNK and MEK/ERK pathways drove cell proliferation and survival in such UM cells. Indeed, according with the synergism between drugs, the combination significantly reduced the expression level of p-c-jun(Ser63), p-Erk1/2 and cyclin D1 to higher extent than each drug alone, as a consequence of Notch1/3 and MEK inhibition. Accordingly the expression level of Hes-1 was further reduced by the combination, while that of p27 was increased, showing that the simultaneous inhibition of MEK and Notch prevented escape mechanisms which are activated once a signaling molecule is inhibited. Both single drug and their combination exerted no significant effect on CDK4/6 and p21 expression level, whereas cobimetinib either alone and in combination led to a significant reduction of Notch2-NTM. Representative immunoblots of cell targets are reported in Fig. 5a (no cropped blots are in Fig. 3-5S), whereas the

quantification of targets expression is summarized in histogram plot (Fig. 5b).

3.5. Combining MEKi and GSI transcriptionally repressed the expression of CCND1, NOTCH1/3 and HES-1

Because of the role of both cyclin D1 and Notch/Hes pathway in cell proliferation and quiescence, we determined, by quantitative real-time PCR, whether the drugs affected their expression levels via transcriptional control. The CCND1 expression data were not consistent with the protein expression profile obtained after treatments; indeed unlike the protein, the mRNA levels were significantly reduced either by single drug and by the combination (*p* < 0.005). However CCND1 expression levels reflected the extent of p-c-Jun(Ser63) decrease after treatments, thus suggesting that the MAPK/JNK pathway exerted a transcriptional control on CCND1 expression, as reported by Bakiri L. et al. [43]. Nirogacestat per se led to a significant decrease of NOTCH-1 (***p* < 0.001) and NOTCH-2/3 receptors mRNAs, though the latter did not reach the significant *p* value. Cobimetinib exerted no effect on Notch receptors mRNA, thus suggesting that MAPK pathway was involved in Notch receptors activation process and not in receptors transcriptional control. However, according with the synergism between drugs, the combination synergistically reduced the mRNA expression of both NOTCH-1 and 3, further supporting the data reported above, which demonstrated a tight cooperation between Notch and MAPK pathways. Of note, only the drugs combination decreased Hes-1 mRNA expression (*p* < 0.005); therefore we can speculate, as already suggested by others [29,30], that a sustained Hes-1 expression in 92.1 cells was likely induced through both a Notch and MAPK-dependent signaling mechanisms. No effect was

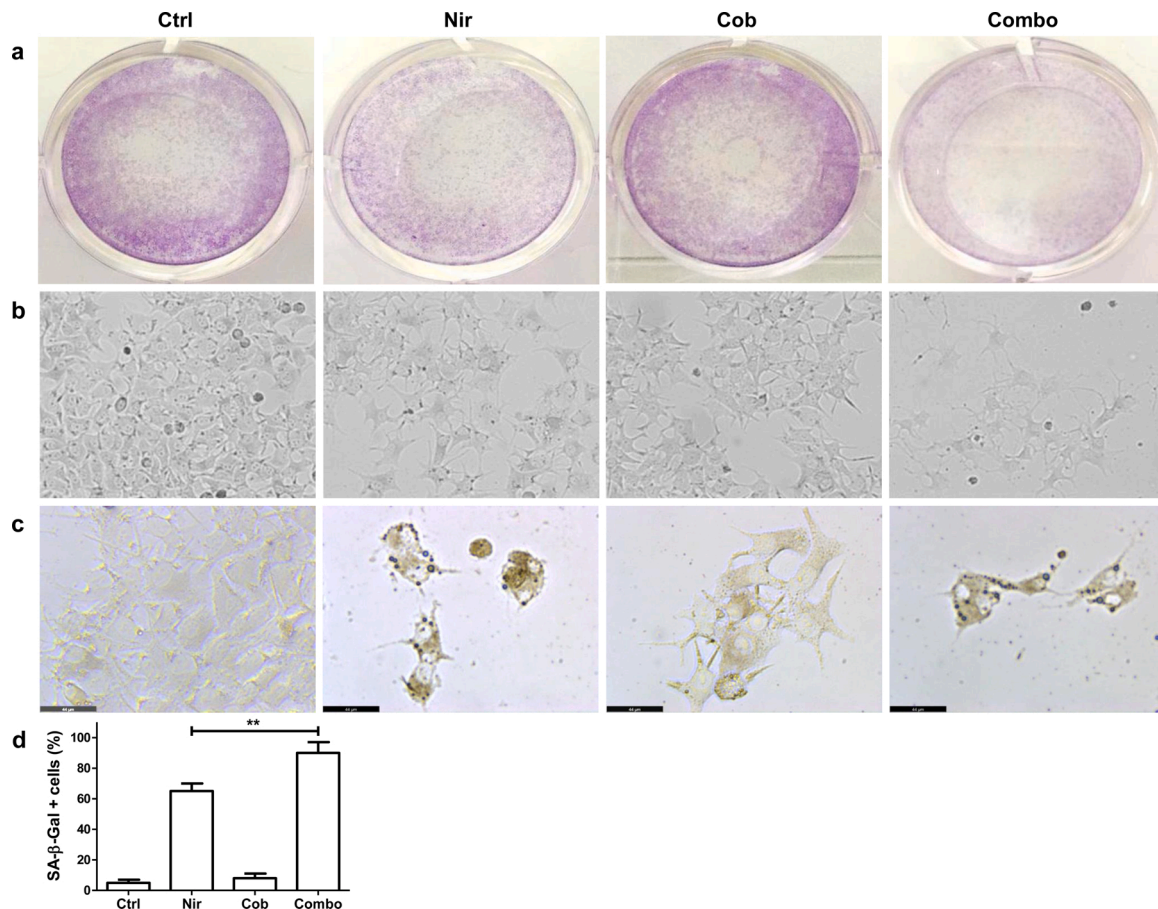


Fig. 4. Senescent-like arrest was induced by the combination of nirogacestat and cobimetinib in UM cells. a. Proliferation of 92.1 cells treated with nirogacestat and/or cobimetinib was evidenced by staining with crystal violet. b. Optical examination of cell morphology showing flattened shaped in nirogacestat and combo-treated cells c. SA-β-Gal staining evidenced as blue color and extensive vacuolization into UM cells treated with nirogacestat and/or cobimetinib. d. Histogram plot reporting the % of SA-β-Gal positive cells. The data reported are means value \pm SD of three independent experiments performed in triplicate, and the significance of difference was analyzed with two tailed *t*-test (***p* < 0.01). All experiments were conducted after exposing cells to drug(s) for 3 days followed by 4 days drug(s) wash out.

observed on Notch 2 transcript, further confirming a satellite role for this receptor in 92.1 cell biology. The levels of mRNAs, normalized to the levels of GAPDH mRNA, are reported as the ratio of mRNA copy number for the gene of interest to mRNA copy number of GAPDH in histograms plot of Fig. 5c.

3.6. Combining MEKi and GSI inhibited 92.1 cells migration towards HepG2 HCC cells

Because 92.1 cells are regarded as a model of UM with high migration/invasion ability, due to the constitutive activation of canonical Notch signaling [42], to study a possible effect of drugs, the cells were harvested and assayed to migrate through a transwell toward the HepG2 cells, that in such assay were utilized as chemoattractant to UM cells. As shown in Fig. 6a, in which are reported representative images of experiments, nirogacestat and cobimetinib alone, revealed a similar moderate efficiency to prevent the migration of UM cells in response to the recall of the chemotactic signals released by HepG2 liver cells. The combination of drugs drastically impaired the ability of the cells to migrate towards HCC cells, according to the significant inhibition of Notch 1/3 receptors activation and Notch 3 transcript level reduction induced by the combination. The quantification of drugs effect, expressed as percentage of vehicle treated cells, is reported in histogram plot in Fig. 6b. Additionally we performed a wound healing assay to further evaluate the inhibitory effect of drug(s) on 92.1 cells migration. To this purpose a wound was created by a straight line across 92.1 confluent monolayer at $t = 0$ h, afterwards the cells were treated with

drug(s) or left untreated (vehicle treated-cells). After 24 h of treatments, the Migration Rate of cells was quantified as described in Material & Methods section, evidencing a reduction in the migration of cells comparable to that found in transwell assay (Fig. 6b).

4. Discussion

To assess the antitumor potential of a combinatorial inhibition of MEK and Notch signaling, cobimetinib and nirogacestat were tested in cutaneous and uveal melanoma cells displaying different Notch and Erk1/2 activation level. The cytotoxicity study revealed that in BRAF^{V600E} MM and GNAQ^{Q209L} UM cells the combination was synergic, thus suggesting for both models a cooperative mechanisms between MAPK and Notch signaling in driving cells proliferation. In BRAF wild type model, the combination was antagonist and became synergic by increasing drugs concentrations, thus suggesting that the cooperation between Notch and MAPK was not crucial for tumor progression. Of note, in sensitive models either the activation level of Erk1/2 and Notch signaling did not correlate with responsiveness to cobimetinib plus nirogacestat. Indeed p-Erk1/2 was mainly activated in BRAF^{V600E} cells and Notch signaling in GNAQ^{Q209L} cells. Hence, because the focus of the study was on the impact of Notch signaling in the response to cobimetinib, we continued our study on GNAQ^{Q209L} UM cells. We found that in such cells, both drugs given alone reduced cell proliferation by inducing apoptosis and in combination synergistically inhibited cell proliferation. However the effect of combining nirogacestat and cobimetinib was the induction of a senescent-like arrest at G0/G1 transition rather than an

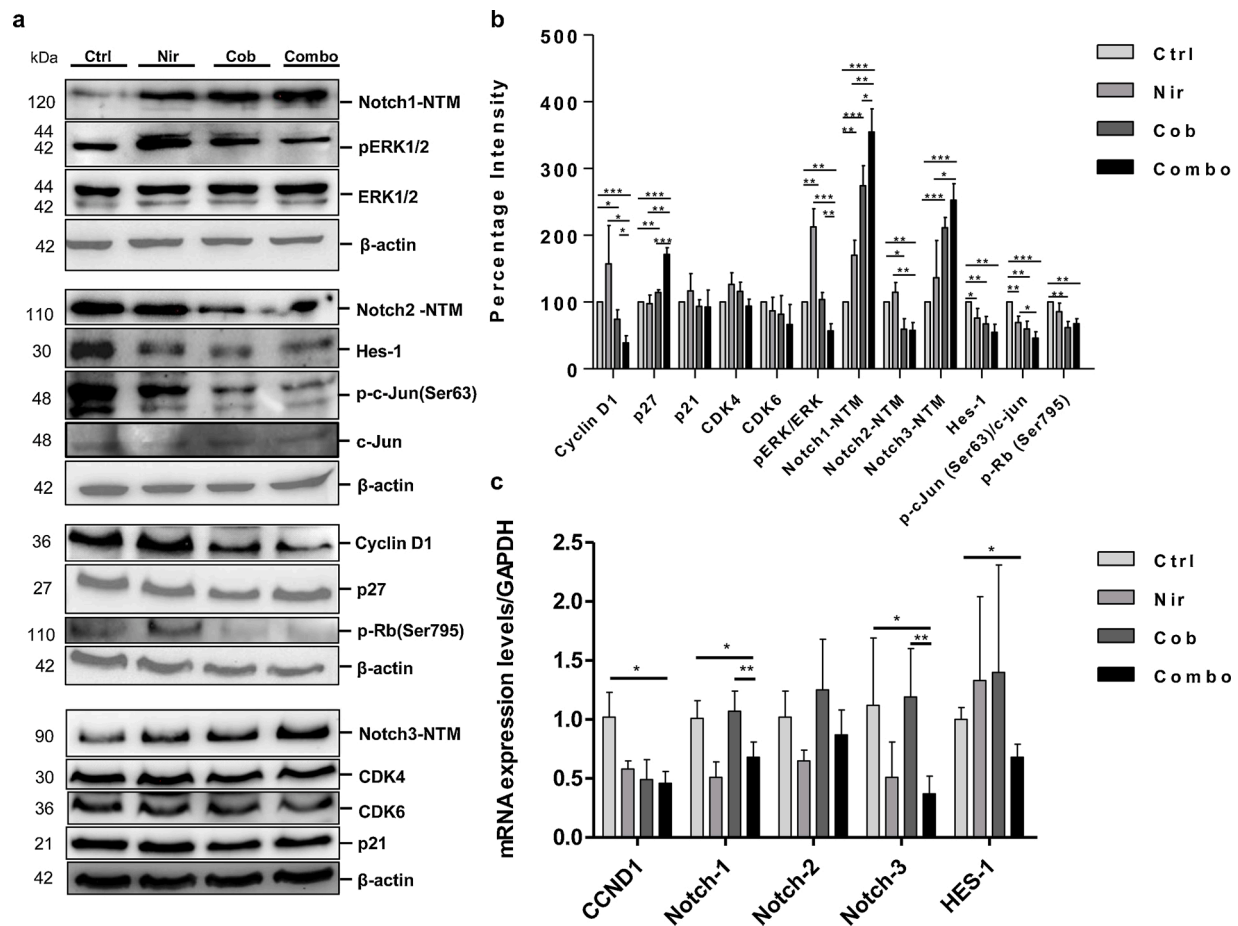


Fig. 5. Combination of nirogacestat and cobimetinib affected cell targets related to cell cycle arrest and proliferation at protein and mRNA level. **a.** Electrophoretic bands of cell targets modulated by drug(s) are showed. **b.** Histogram plot summarizing the percentage intensity of bands. β -actin was used as loading control. The data are presented as the mean \pm SD ($n = 3$) and the two-tailed t -test was used to analyze the difference between targets expression in combination treated cells vs each drug alone and in single drug and in combination treated cells vs vehicle treated cells (Ctrl) (* $p < 0.05$, ** $p < 0.01$ and *** $p < 0.001$). **c.** Real-time RT-PCR assay was applied to detect the expression of cyclin D1, Notch 1/3 and HES-1 according to the use of single drug or drugs combination. GAPDH was used as housekeeping gene. The data are presented as the mean \pm SD of three independent experiments. The significance of difference in mRNA expression level of target genes was analyzed with two tailed t -test (* $p < 0.05$ and ** $p < 0.01$).

increase in apoptosis, suggesting that the constitutive activation of Notch not only promotes tumor growth but it also allows the escape from senescence in such cells, once MEK is targeted. The induction of senescence was reflected in the transcriptional downregulation of cyclin D1, reduced phosphorylation of RB and increased expression of p27. Accordingly Zhu et al. [32] demonstrated that the downregulation of cyclin D1 and the reduction of RB phosphorylation were associated to the senescent phenotype induced by the addition of GSI to BRAFi in BRAF-mutated cutaneous melanoma cells. Of note, we observed that the administration of cobimetinib, at tested concentration, did not inhibit p-Erk1/2, instead it resulted in a strong inhibition of the JNK downstream target c-jun, highlighting a preferential activation of MEK/c-Jun N-terminal kinase (JNK) signaling in 92.1 cells. Nirogacestat as well, even though to a lesser extent than cobimetinib, inhibited c-jun activation but induced a feedback activation of Erk1/2; perhaps because c-jun was inhibited. Albeit the results on Erk1/2 and c-jun seem to be in contrast with research reports showing that in GNAQ^{Q209L} UM cells c-jun is induced by MEK inhibition [43], and that characteristically GSI exerts antitumor effect by inhibiting Erk1/2 activation in cutaneous melanoma [32]; it is known that G protein-mediated signaling involves a complex network of binding partners and effectors proteins. Therefore it is conceivable that in 92.1 cells, GNAQ^{Q209L} triggered a route that involved the MEK/JNK/ERK1/2 pathway to engage Notch signaling and boosting proliferation, migration and prevention of cell senescence.

Another evidence supporting our hypothesis was that even cobimetinib inhibited Notch1/3 activation and Hes-1 expression, that is known to play a crucial role in the inhibition of senescence in normal and in tumor cells. Hence only a combined inhibition of Notch and MEK prevented escape mechanisms that were activated once a signaling molecule was targeted in such cells. Although further studies are required to delineate the precise mechanisms by which the MAPK pathway promoted Notch signaling, to the best of our knowledge this is the first time that a combination targeting MAPK and Notch signaling has been experienced in GNAQ^{Q209L} UM cells, pointing out possible mechanisms underlying the MEKi failure in UM treatment [44] and lending credence to the notion that a crosstalk between MAPK and Notch signaling promotes tumorigenesis and disease progression. Although we are aware that this combination has been tested only in a UM model, we also know that this is a rare tumor, thus each molecular subtype may have unique clinical characteristics and may respond best to a specific therapeutic strategy, as reported by other authors [32], that should be identified and developed through tailored clinical trials.

5. Conclusions

Main finding of the present study is that the combined targeting of Notch and MAPK pathway was synergic either in BRAF^{V600E} MM model and GNAQ^{Q209L} UM model. Remarkably, UM is little responsive to MEK

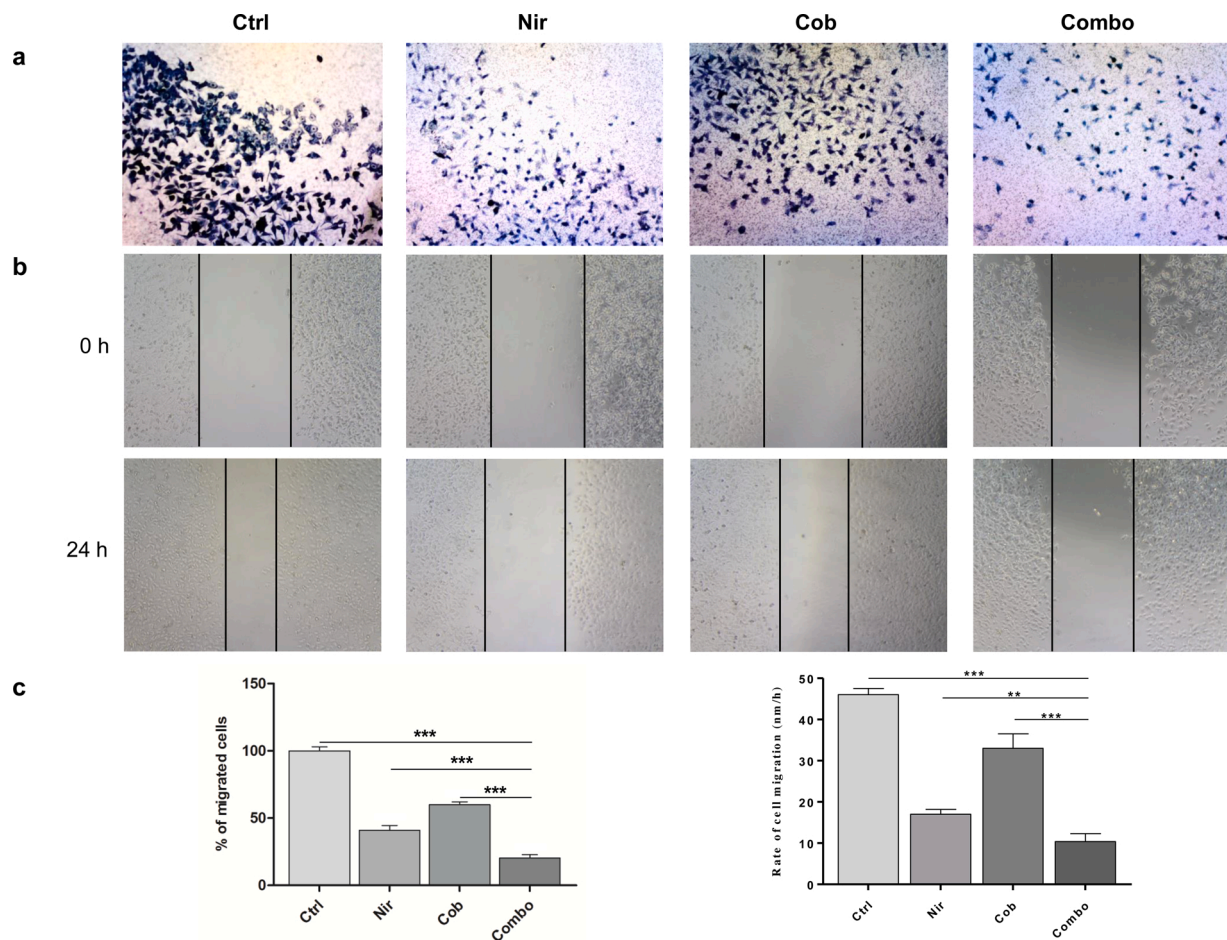


Fig. 6. Nirogacestat and/or cobimetinib repressed the migration of 92.1 cells. a. Representative images showing transwell migration assay of 92.1 uveal melanoma cell line towards HepG2 HCC cells, after each drug given alone and drugs combination. Cells are stained with Diff-Quick. b. Representative images showing the effect of drug(s) on 92.1 cell line migration, performed by Wound Healing assay. c. Histograms plot reporting the quantification of cells migration in each condition. Data reported are means ($n = 3$) \pm SD from three independent experiments. Two-tailed *t*-test was used to analyze the difference between the combination treatment and each drug given alone or between the combination treatment versus vehicle treated cells (Ctrl). (** $p < 0.01$, *** $p < 0.001$).

inhibition, however no scientific reports dissecting the molecular mechanisms contributing to MEKi failure in UM patients are available. Here, we showed that in GNAQ^{Q209L} UM cells a coordinate interplay between MAPK and Notch signaling triggered proliferation, migration and prevented cell senescence, thus suggesting a role for Notch in the resistance to MEKi. Although this is a pilot study in UM, we demonstrated that the simultaneous inhibition of Notch and MAPK pathways prolonged the treatment efficacy of MEKi in such cells, suggesting that this approach warrants further investigation.

Funding

This research was funded by Ricerca Corrente 2018-2020 “Meccanismi e strategie per superare la farmacoresistenza alla terapia target-oriented o all’immunoterapia nel melanoma metastatico” (Italian Ministry of Health).

Declaration of Competing Interest

The authors declare no conflict of interest.

Acknowledgments

The authors acknowledge Prof. Marco Ragusa (Department of Biomedical and Biotechnological Sciences, Section of Biology and

Genetics G. Sichel, University of Catania, Catania, 95123, Italy and Oasi Research Institute - IRCCS, Troina, 94018, Italy) who generously gifted 92.1 cell line that was obtained from the Interlab Cell Line Collection (ICLC), an International Certified Repository Authority within the IRCCS Azienda Ospedaliera Universitaria San Martino-IST (Istituto Nazionale per la Ricerca sul Cancro, Italy).

Appendix A. Supplementary data

Supplementary material related to this article can be found, in the online version, at doi:<https://doi.org/10.1016/j.biopha.2020.111006>.

References

- [1] Z. Wei, H.T. Liu, MAPK signal pathways in the regulation of cell proliferation in mammalian cells, *Cell Res.* 12 (2002) 9–18, <https://doi.org/10.1038/sj.cr.7290105>.
- [2] C. Widmann, S. Gibson, M.B. Jarpe, G.L. Johnson, Mitogen-activated protein kinase: conservation of a three-kinase module from yeast to human, *Physiol. Rev.* 79 (1999) 143–180, <https://doi.org/10.1152/physrev.1999.79.1.143>.
- [3] R. Buscà, R. Ballotti, Cyclic AMP a key messenger in the regulation of skin pigmentation, *Pigment Cell Res.* 13 (2000) 60–69, <https://doi.org/10.1034/j.1600-0749.2000.130203.x>.
- [4] P.M. Dantonio, M.O. Klein, M.R.V.B. Freire, C.N. Araujo, A.C. Chiacetti, R. G. Correa, Exploring major signaling cascades in melanomagenesis: a rationale route for targeted skin cancer therapy, *Biosci. Rep.* 38 (2018), <https://doi.org/10.1042/BSR20180511>.

- [5] R.A.N. Johnpulle, D.B. Johnson, J.A. Sosman, Molecular targeted therapy approaches for BRAF wild-type melanoma, *Curr. Oncol. Rep.* 18 (2016) 1–8, <https://doi.org/10.1007/s11912-015-0485-6>.
- [6] A.Y. Bedikian, Metastatic uveal melanoma therapy: current options, *Int. Ophthalmol. Clin.* 46 (2006) 151–166, <https://doi.org/10.1097/01.iio.0000195852.08453.de>.
- [7] J.J. Park, R.J. Diefenbach, A.M. Joshua, R.F. Kefford, M.S. Carlino, H. Rizos, Oncogenic signaling in uveal melanoma, *Pigment Cell Melanoma Res.* 31 (2018) 661–672, <https://doi.org/10.1111/pcmr.12708>.
- [8] J. Yang, D.K. Manson, B.P. Marr, R.D. Carvajal, Treatment of uveal melanoma: where are we now? *Ther. Adv. Med. Oncol.* 10 (2018) <https://doi.org/10.1177/1758834018757175>, 175883401875717.
- [9] M.D. Onken, L.A. Worley, M.D. Long, S. Duan, M.L. Council, A.M. Bowcock, J. W. Harbour, Oncogenic mutations in GNAQ occur early in uveal melanoma, *Investig. Ophthalmol. Vis. Sci.* 49 (2008) 5230–5234, <https://doi.org/10.1167/iovs.08-2145>.
- [10] C.D. Van Raamsdonk, K.G. Griewank, M.B. Crosby, M.C. Garrido, S. Vemula, T. Waisner, A.C. Obenaus, W. Wackernagel, G. Green, N. Bouvier, M.M. Sozen, G. Baimukanova, R. Roy, A. Heguy, I. Dolgalev, R. Khanin, K. Busam, M. R. Speicher, J. O'Brien, B.C. Bastian, Mutations in GNA11 in uveal melanoma, *N. Engl. J. Med.* 363 (2010) 2191–2199, <https://doi.org/10.1056/NEJMoa1000584>.
- [11] C.D. Van Raamsdonk, V. Bezroukove, G. Green, J. Bauer, L. Gaugler, J.M. O'Brien, E.M. Simpson, G.S. Barsh, B.C. Bastian, Frequent somatic mutations of GNAQ in uveal melanoma and blue naevi, *Nature.* 457 (2009) 599–602, <https://doi.org/10.1038/nature07586>.
- [12] M. O'Hayre, J. Vázquez-Prado, I. Kufareva, E.W. Stawiski, T.M. Handel, S. Seshagiri, J.S. Gutkind, The emerging mutational landscape of G proteins and G-protein-coupled receptors in cancer, *Nat. Rev. Cancer* 13 (2013) 412–424, <https://doi.org/10.1038/nrc3521>.
- [13] A.N. Shoushtari, R.D. Carvajal, GNAQ and GNA11 mutations in uveal melanoma, *Melanoma Res.* 24 (2014) 525–534, <https://doi.org/10.1097/CMR.0000000000000121>.
- [14] T.E. Schank, J.C. Hassel, Immunotherapies for the treatment of uveal melanoma—history and future, *Cancers (Basel)*. 11 (2019), <https://doi.org/10.3390/cancers11081048>, 1048.
- [15] Z. Wang, Y. Li, A. Ahmad, A.S. Azmi, S. Banerjee, D. Kong, F.H. Sarkar, Targeting Notch signaling pathway to overcome drug resistance for cancer therapy, *Biochim. Biophys. Acta - Rev. Cancer.* 1806 (2010) 258–267, <https://doi.org/10.1016/j.bbcan.2010.06.001>.
- [16] C.C. Pinnix, J.T. Lee, Z.J. Liu, R. McDaid, K. Balint, L.J. Beverly, P.A. Brafford, M. Xiao, B. Himes, S.E. Zabierowski, Y. Yashiro-Ohtani, K.L. Nathanson, A. Bengston, P.M. Pollock, A.T. Weeraratna, B.J. Nickoloff, W.S. Pear, A. J. Capobianco, M. Herlyn, Active Notch1 confers a transformed phenotype to primary human melanocytes, *Cancer Res.* 69 (2009) 5312–5320, <https://doi.org/10.1158/0008-5472.CAN-08-3767>.
- [17] S. Artavanis-Tsakonas, M.D. Rand, R.J. Lake, Notch signaling: cell fate control and signal integration in development, *Science (80-)* 284 (1999) 770–776, <https://doi.org/10.1126/science.284.5415.770>.
- [18] M. Osawa, D.E. Fisher, Notch and Melanocytes: Diverse Outcomes from a Single Signal, *J. Invest. Dermatol.* 128 (2008) 2571–2574, <https://doi.org/10.1038/jid.2008.289>.
- [19] L. Asnaghi, K.B. Ebrahimi, K.C. Schreck, E.E. Bar, M.L. Coonfield, W.R. Bell, J. Handa, S.L. Merbs, J.W. Harbour, C.G. Eberhart, Notch signaling promotes growth and invasion in uveal melanoma, *Clin. Cancer Res.* 18 (2012) 654–665, <https://doi.org/10.1158/1078-0432.CCR-11-1406>.
- [20] B. Bedogni, Notch signaling in melanoma: interacting pathways and stromal influences that enhance Notch targeting, *Pigment Cell Melanoma Res.* 27 (2014) 162–168, <https://doi.org/10.1111/pcmr.12194>.
- [21] H. Liu, C. Lei, K. Long, X. Yang, Z. Zhu, L. Zhang, J. Liu, Mutant GNAQ promotes cell viability and migration of uveal melanoma cells through the activation of Notch signaling, *Oncol. Rep.* 34 (2015) 295–301, <https://doi.org/10.3892/or.2015.3949>.
- [22] S.E. Coupland, S.L. Lake, B. Damato, Molecular pathology of uveal melanoma. *Clin. Ophthalmic Oncol. Uveal Tumors*, Springer, Berlin Heidelberg, Berlin, Heidelberg, 2014, pp. 125–136, https://doi.org/10.1007/978-3-642-54255-8_10.
- [23] S.J. Bray, Notch signalling in context, *Nat. Rev. Mol. Cell Biol.* 17 (2016) 722–735, <https://doi.org/10.1038/nrm.2016.94>.
- [24] P. Ranganathan, K.L. Weaver, A.J. Capobianco, Notch signalling in solid tumours: a little bit of everything but not all the time, *Nat. Rev. Cancer* 11 (2011) 338–351, <https://doi.org/10.1038/nrc3035>.
- [25] L. Tamagnone, S. Zacchigna, M. Rehman, Taming the Notch transcriptional regulator for cancer therapy, *Molecules.* 23 (2018) 431, <https://doi.org/10.3390/molecules23020431>.
- [26] S. Weijzen, P. Rizzo, M. Braid, R. Vaishnav, S.M. Jonkheer, A. Zlobin, B.A. Osborne, S. Gottipati, J.C. Aster, W.C. Hahn, M. Rudolf, K. Siziopikou, W.M. Kast, L. Miele, Activation of Notch-1 signaling maintains the neoplastic phenotype in human Ras-transformed cells, *Nat. Med.* 8 (2002) 979–986, <https://doi.org/10.1038/nm754>.
- [27] K. Fitzgerald, A. Harrington, P. Leder, Ras pathway signals are required for notch-mediated oncogenesis, *Oncogene.* 19 (2000) 4191–4198, <https://doi.org/10.1038/sj.onc.1203766>.
- [28] S. Mittal, A. Sharma, S.A. Balaji, M.C. Gowda, R.R. Dighe, R.V. Kumar, A. Rangarajan, Coordinate hyperactivation of notch1 and Ras/MAPK pathways correlates with poor patient survival: novel therapeutic strategy for aggressive breast cancers, *Mol. Cancer Ther.* 13 (2014) 3198–3209, <https://doi.org/10.1158/1535-7163.MCT-14-0280>.
- [29] I. Tremblay, E. Paré, D. Arseneault, M. Douziech, M.J. Boucher, The MEK/ERK pathway promotes NOTCH signalling in pancreatic cancer cells, *PLoS One* 8 (2013) e85502, <https://doi.org/10.1371/journal.pone.0085502>.
- [30] Y. Nishikawa, Y. Kodama, M. Shiokawa, T. Matsumori, S. Marui, K. Kuriyama, T. Kuwada, Y. Sogabe, N. Kakiuchi, T. Tomono, A. Mima, T. Morita, T. Ueda, M. Tsuda, Y. Yamauchi, Y. Sakuma, Y. Ota, T. Maruno, N. Uza, M. Uesugi, R. Kageyama, T. Chiba, H. Seno, Hes1 plays an essential role in Kras-driven pancreatic tumorigenesis, *Oncogene.* 38 (2019) 4283–4296, <https://doi.org/10.1038/s41388-019-0718-5>.
- [31] C.A. Martz, K.A. Ottina, K.R. Singleton, J.S. Jasper, S.E. Wardell, A. Peraza-Penton, G.R. Anderson, P.S. Winter, T. Wang, H.M. Alley, L.N. Kwong, Z.A. Cooper, M. Tetzlaff, P.L. Chen, J.C. Rathmell, K.T. Flaherty, J.A. Wargo, D.P. McDonnell, D. M. Sabatini, K.C. Wood, Systematic identification of signaling pathways with potential to confer anticancer drug resistance, *Sci. Signal.* 7 (2014), <https://doi.org/10.1126/scisignal.aaa1877> ra121–ra121.
- [32] G. Zhu, X. Yi, S. Haferkamp, S. Hesbacher, C. Li, M. Goebeler, T. Gao, R. Houben, D. Schrama, Combination with γ -secretase inhibitor prolongs treatment efficacy of BRAF inhibitor in BRAF-mutated melanoma cells, *Cancer Lett.* 376 (2016) 43–52, <https://doi.org/10.1016/j.canlet.2016.03.028>.
- [33] C. Krepler, M. Xiao, M. Samanta, A. Vultur, H.Y. Chen, P. Brafford, P.I. Reyes-Urube, M. Halloran, T. Chen, X. He, D. Hristova, Q. Liu, A.A. Samatar, M.A. Davies, K.L. Nathanson, M. Fukunaga-Kalabis, M. Herlyn, J. Villanueva, Targeting Notch enhances the efficacy of ERK inhibitors in BRAFV600E melanoma, *Oncotarget.* 7 (2016) 71211–71222, <https://doi.org/10.18632/oncotarget.12078>.
- [34] P. Zanna, I. Maida, C. Grieco, S. Guida, M.C. Turpin Sevilla, S. De Summa, S. Tommasi, G.A. Vena, R. Filotico, G. Guida, Three novel human sporadic melanoma cell lines: signaling pathways controlled by MC1R, BRAF and β -catenins, *J. Biol. Regul. Homeost. Agents* 27 (2013) 131–141.
- [35] F. Dituri, A. Mazzocca, L. Lupo, C.E. Edling, A. Azzariti, S. Antonaci, M. Falasca, G. Giannelli, PI3K class IB controls the cell cycle checkpoint promoting cell proliferation in hepatocellular carcinoma, *Int. J. Cancer* 130 (2012) 2505–2513, <https://doi.org/10.1002/ijc.26319>.
- [36] R.M. Iacobozzi, P. Letizia, L.A. Assunta, L. Valentino, L. Antonio, C. Annalisa, A. Emiliano, D.F. Roberta, A. Amalia, F. Massimo, D. Nunzio, Targeting human liver cancer cells with lactobionic acid-G(4)-PAMAM-FITC sorafenib loaded dendrimers, *Int. J. Pharm.* 528 (2017) 485–497, <https://doi.org/10.1016/j.ijpharm.2017.06.049>.
- [37] T.C. Chou, Drug combination studies and their synergy quantification using the chou-talalay method, *Cancer Res.* 70 (2010) 440–446, <https://doi.org/10.1158/0008-5472.CAN-09-1947>.
- [38] L. Porcelli, R.M. Iacobozzi, R. Di Fonte, S. Serrati, A. Intini, A.G. Solimando, O. Brunetti, A. Calabrese, F. Leonetti, A. Azzariti, N. Silvestris, CAFs and TGF- β signaling activation by mast cells contribute to resistance to Gemcitabine/Nabpaclitaxel in Pancreatic Cancer, *Cancers (Basel)*. 11 (2019) 330, <https://doi.org/10.3390/cancers11030330>.
- [39] A. Grada, M. Otero-Vinas, F. Prieto-Castrillo, Z. Obagi, V. Falanga, Research Techniques Made Simple: Analysis of Collective Cell Migration Using the Wound Healing Assay, *J. Invest. Dermatol.* 137 (2017), <https://doi.org/10.1016/j.jid.2016.11.020> e11–e16.
- [40] F. Rodier, J. Campisi, Four faces of cellular senescence, *J. Cell Biol.* 192 (2011) 547–556, <https://doi.org/10.1083/jcb.201009094>.
- [41] S. Goel, M.J. DeCristo, S.S. McAllister, J.J. Zhao, CDK4/6 inhibition in Cancer: beyond cell cycle arrest, *Trends Cell Biol.* 28 (2018) 911–925, <https://doi.org/10.1016/j.tcb.2018.07.002>.
- [42] L. Asnaghi, J.T. Handa, S.L. Merbs, J.W. Harbour, C.G. Eberhart, A role for Jag2 in promoting uveal melanoma dissemination and growth, *Investig. Ophthalmol. Vis. Sci.* 54 (2013) 295–306, <https://doi.org/10.1167/iovs.12-10209>.
- [43] L. Bakiri, Cell cycle-dependent variations in c-Jun and JunB phosphorylation: a role in the control of cyclin D1 expression, *EMBO J.* 19 (2000) 2056–2068, <https://doi.org/10.1093/emboj/19.9.2056>.
- [44] T. Steeb, A. Wessely, T. Ruzicka, M.V. Heppt, C. Berking, How to MEK the best of uveal melanoma: a systematic review on the efficacy and safety of MEK inhibitors in metastatic or unresectable uveal melanoma, *Eur. J. Cancer* 103 (2018) 41–51, <https://doi.org/10.1016/j.ejca.2018.08.005>.